

Investigation on the spatial evolution of the emission spectra in laser-induced Ni plasmas

Chuan-Mei Du^{a,*}, Ming-Xu Zhang^b, and Ying Xu^a

^a School of Civil Engineering and Architecture, Anhui University of Science and Technology, Huainan, Anhui 232001, China

^b School of Materials Science and Engineering, Anhui University of Science and Technology, Huainan, Anhui 232001, China

Received 28 March 2012; Accepted (in revised version) 30 April 2012

Published Online 28 March 2013

Abstract. The spatial resolved emission spectrum of Ni atom in laser induced Ni plasma is measured in the wavelength region from 350 nm to 600 nm. The spatial evolution of the relative intensities and the Stark broadening of the 385.83 nm emission spectrum lines are also obtained. It is shown that Stark broadening and intensity of the spectrum lines increases firstly to its maximum and then decreases along the direction of laser beam when the distance from the target surface is in the range from 0 to 2.5 mm. The maximum value of Stark broadening and relative intensity of the spectrum lines appear at 1.5 mm from the target surface.

PACS: 32.80.Qk, 32.70.Jz

Key words: laser induced Ni plasma, emission spectra, the spatial resolved emission spectrum, Stark broadening

1 Introduction

In the many researching means, the diagnosis technology of plasma emission spectra is widely used with its simply operation and without interference characters for the plasma. People have given a lot of information about the plasma with this technology, such as the mechanism of plasma generation(including the process of breakdown, the laser indignation combustion and detonation) and its thermodynamic characters(electronic density, the stimulate temperature and the macro expansion and so on)[1,2]. It can obtain the different compositions and the evolution features of the state in the plasma with the measured time and spatial resolved spectra, can help the people to understand the formation and expanding rule of plasma plume and reflect the state change of the excited atom and

*Corresponding author. *Email address:* ducml997@126.com (C. -M. Du)

ions. It is especially important for us to understand the physical and chemical characters of the ablation process, also is the most concerned content in the material vapor deposition. Although there have many reports about the research of the laser induced plasma emission spectra in the literatures [3-19], is basically based on the study of the time evolution emission spectra and is less for the spatial evolution emission spectral. Ma *et al.* studied the interaction of the aluminum plasma plume and argon through the research of the time and spatial resolved emission spectra, the results show that in the plasma center there have plenty of argon and aluminum plasma plume mixed [20]. Zorba *et al.* analyzed the spatial resolved emission spectra using femtosecond laser-induced breakdown spectroscopy and realized the high spatial resolution chemical analysis [21]. We measure the spatial resolved emission spectra of Ni atom in the plasma ablated by the laser, the relative intensity of the emission spectra and the change character of the Stark broadening with the radial distance using the 532nm laser to ablate Ni target.

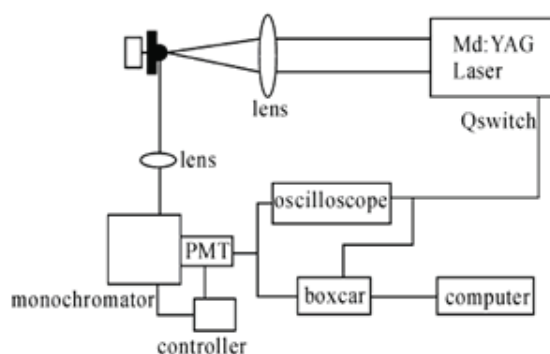


Figure 1: Diagram of the experimental setup.

2 Experimental

A schematic diagram of the experimental set-up is shown in Fig. 1, the laser sources for ablation is 532 nm output of YAG laser(Spectra-Physics, LAB170-10), repetition frequency 10HZ, pulse width 7ns, beam diameter 6 mm, Mono-pulse laser energy (532 nm) in the range of 2-300mJ can be adjusted. The pulse laser beam is focused to the surface of the Ni target using a quartz lens with 100 mm nominal focal length, the focus in the samples from the sample surface is about 2 mm, so you can get the best plasma emission spectra signal. In order to ensure that each laser pulse rips into the different target position, with slow rotation motor (1R/min) controlling samples for low speed rotation. Samples are in the atmospheric environment. In the vertical direction with the laser beam and the parallel direction with samples, the laser plasma emission spectra signal was coupled to the entrance slit of monochromator (ACTON, SP-2750) with the 70 mm focal length lens combination the two times imaging amplification. The imaging lens was placed on one

dimensional adjustable frame with precision adjustment, in the vertical direction with the ablation laser beam the adjustable precision is 10 m, the resolution rate of the monochromator is 0.023 nm, the entrance slit width is 80 m, the spectroscopy signal after through the monochromator is detected, collected and processed by the photomultiplier tubes (R376), Boxcar average implement and computer. The output signal from photomultiplier tubes is monitored through digital storage oscilloscopes (TEK460A), BOXCAR and oscilloscope are triggered by synchronization output pulse of YAG laser Q switch. By adjusting the delay time of BOXCAR sampling gate, it can determine the emission spectra signal in different time at the process of the laser plasma formation. In experiment, the sampling gate width 60 ns, sampling time 30, sensitivity 50mV. The standard Ni samples used in the experiments is provided by the Alfa Aesar company, in which the content of Ni was 99.5%.

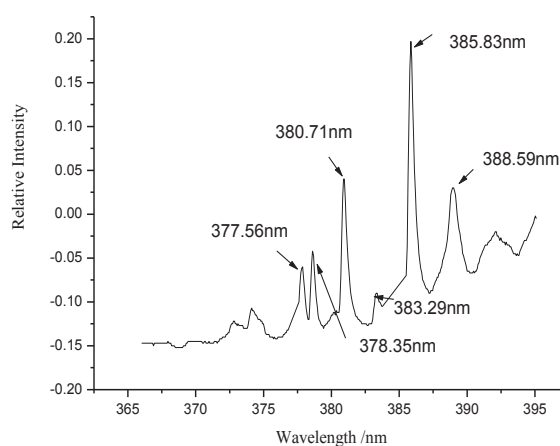


Figure 2: The emission spectra from 365 to 395nm of Ni atom in the plasma.

3 Results and discussion

3.1 Measurement and adscription of emission spectrum for Ni atom

In the dynamic research about the laser induced nickel plasma emission spectra, Kodama team studied the relationship between the nickel atomic emission spectra with the laser energy [22], when the laser energy was about 5eV the spectrum intensity of the nickel atom grew dramatically. Kazuaki *et al.* studied the spectrum character of nickel ion in different buffer gas (argon and krypton gas) [23], the experimental results show that the nickel ion spectrum is different in two buffer gas. We focus on the emission spectrum of nickel atom in the range of 365-395 nm in the plasma with the laser ablation Ni target, get and ascribe the six spectral lines.

Our previous experimental results showed that the laser induced nickel plasma spec-

Table 1: The energy levels of the transitions of Ni atom measured in the experiment.

Experimental spectral lines	The corresponding transition energy level
Ni I 377.56 nm	$3d^9(^2D)4s-3d^9(^2D)4p$
Ni I 378.35 nm	$3d^9(^2D)4s-3d^9(^2D)4p$
Ni I 380.71 nm	$3d^9(^2D)4s-3d^9(^2D)4p$
Ni I 383.29 nm	$3d^8(^3F)4s^2-3d^8(^3F)4s4p(^3P^*)$
Ni I 385.83 nm	$3d^9(^2D)4s-3d^9(^2D)4p$
Ni I 388.59 nm	$3d^8(^3F)4s-3d^8(^3F)4s$

tral relative intensity reached the maximum when the delay time in detection was 300 ns, so in this experiment, we use single pulse laser energy with 24mJ, the detection delay time 300 ns, in the range of 365-395 nm, in the place of 1.5 mm from the target surface, the measured plasma spectrum is shown as in Fig. 2. In this spectrum range, we observe six nickel atomic spectrum lines, corresponding wavelength is 377.56 nm, 378.35 nm, 380.71 nm, 383.29 nm, 385.83 nm and 388.59 nm, the transition energy level corresponding these spectral lines is shown in Table 1.

3.2 Measurement of the spatial resolved emission spectrum

It can obtain the rich dynamic information about the formation process of the laser plasma from the spatial resolved spectrum measured in the experiment and help people to recognize the rule of the plasma plume formation and inflation. Mitchel firstly reported the emission spectra of Al target ablated by CO₂ laser in vacuum and atmospheric conditions respectively [24]. Knudtson researched the time and spatial resolved spectrum of Al plasma with the dye laser pumped by the flash lamp [25]. Su *et al.* carried on the research of the emission spectrum of Cu plasma ablated by the laser in the air [26]. In our investigated literatures it has not been seen the study of the Ni plasma spatial resolved spectra in the range of 365-395 nm. So we make research on the spatial resolved character of the Ni plasma emission spectra in the range of 384.5 nm - 386.5 nm and 379.5 nm-381.5 nm using the laser with the wavelength 532 nm.

In Fig. 3, the Ni atomic emission spectrum of the plasma in the different radial distance are obtained in the range of 384.5 nm - 386.5 nm and 379.5 nm - 381.5 nm, with the single pulse laser energy 24mJ, the detection delay time 300 ns.

It can be seen from Fig. 3 that there are mainly the continuous spectrum near the target, also with the weak atomic spectrum. In the range of 2.5 mm from the target surface, there are very strong continuous spectrum distribution, on the which are the discrete atomic spectral lines, besides, it is shown that the continuous spectrum intensity increases firstly and then decreases with the distance from the target surface increasing,

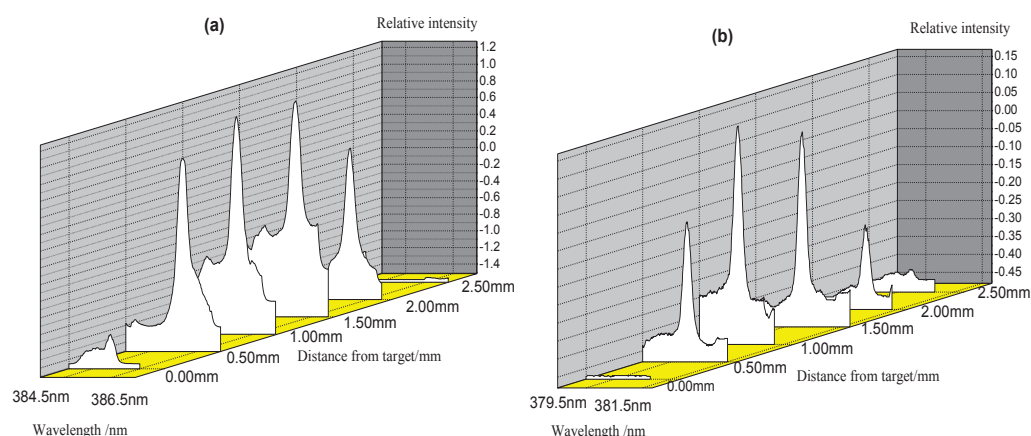


Figure 3: Spatial-evolution of Ni spectral line at 385.83nm (a) and 380.71nm (b) respectively .

we think it is the result of the complex radiation interaction with the bremsstrahlung. The continuous spectrum is generated owing to the electrons bremsstrahlung and the composite process of ions and electrons. Along with the increase of distance from the target surface, it make the atoms ionization further strengthen with the energy transfer and conversion caused by the laser energy absorption and electrons colliding. The continuous radiation gradually strengthen due to the recombination of ions strengthening gradually with the ion density increasing in the plasma. At the same time, the enhancement of the electron bremsstrahlung cause the continuous spectrum intensity observed in experiment to augment with the distance from the target surface increasing, but with the distance from the target surface further increasing, due to the expansion movement of the plasma in the space and make the ion density in the plasma decrease, it lead to reduce for the property of the electron and ions composite and cause bremsstrahlung lower. Simultaneously, with the mean free path of the electron increasing, it induce the probability of collision to decline, bremsstrahlung also get weak. The common function lead to the result in the experiment, the continuous spectrum intensity increases firstly and then decreases with the distance from the target surface increasing when the distance from target surface increase to the certain value.

We can get that discrete spectrum intensity changing with the distance has similar with continuous spectrum in Fig. 3, it is decided by the dynamic character of the excited atom in the laser plasma. With the distance from the target surface increasing near target surface, the ionization atom is more strengthen for the energy transfer and conversion due to the laser energy absorbing and the electron colliding. When the electron density in the plasma build up, the probability of the atom locating in the excited state increase for inelastic collision between the electron with the neutral atoms. With the distance further increasing, for the plasma spreading, the atom density decrease in no time, it causes the atom spectrum intensity decrease with the distance increasing. In addition we can see the line diameter of the plasma in the experiment is about 2.5 mm from the Fig. 3.

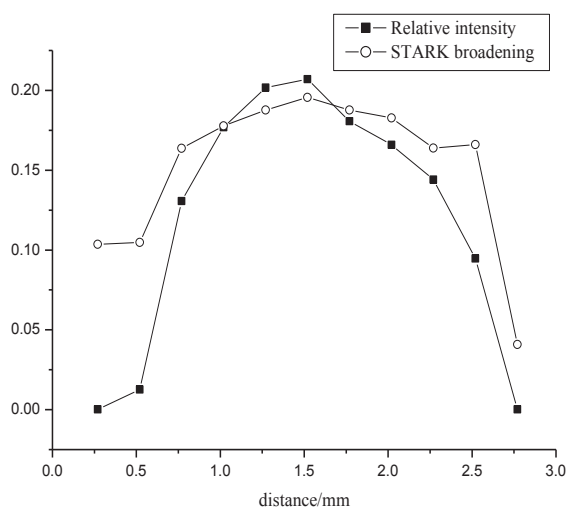


Figure 4: The spatial evolution of the relative intensity and the STARK broadening of 385.83nm spectra line.

3.3 The spatial evolution character of the spectrum relatively intensity and Stark broadening

By the description of the spectrum broadening, it is known that in this experimental condition the laser plasma emission spectrum lines broadening depend on the Stark broadening, other broadening can be ignored. Through the previous experimental results showed that in the long delay time the width of the laser induce plasma emission spectra have no change basically with the delay time increasing, at same time, the time for the plasma emission spectra existing change shorter with the pressure of buffer gas increasing [27]. Thus the laser induced plasma emission spectra exit very short in the atmospheric environment as expected, in this experiment the time of the laser plasma emission spectrum existing is about $1\mu\text{s}$ and far less than the time of the laser plasma emission spectrum existing in vacuum ($10\mu\text{s}$). So we can get the numerical value for Stark broadening in this delay time through measuring the difference of the width between in a certain delay time with the delay time $1.1\mu\text{s}$. The single pulse laser energy is 24mJ, the detection delay time 300 ns, the spectral relative intensity for Ni atom at 385.83 nm and Stark broadening, the variation character with the radial distance is shown in Fig. 4.

It is shown from Fig. 4 that Stark broadening and intensity of the spectral lines increases firstly to its maximum and then decreases along the direction of laser beam when the distance from the target surface increase. The maximum value of Stark broadening and relative intensity of the spectral lines appear at 1.5 mm from the target surface, it illuminate that in this area the electron density is maximum, this lead to get the maximum excited probability for the inelastic collision between atom with electron, thus, make the atom spectrum intensity to reach the maximum value. At the same time, the variation character of the atom spectrum intensity with the distance is similar with the continuous

spectrum, it also confirm that the conclusion is consistent by different methods. Our later measurement results for the plasma electron density also confirm this conclusion.

4 Conclusion

The laser induced Ni plasma emission spectra at 532 nm is obtained in the experiment, in Ni plasma spectrum in the range of 365 nm - 395 nm , the six Ni atom spectrum lines are observed, the corresponding wavelength is 377.56 nm, 378.35 nm, 380.71 nm, 383.29 nm, 385.83 nm and 388.59 nm. The single pulse laser energy is 24mJ, the detection delay time 300 ns, the spatial evolution spectrum for Ni atom at 385.83 nm is measured, the results show that the continuous spectrum relative intensity and discrete spectrum relative intensity increases firstly and then decreases with the distance from the target surface increasing, it is the result of interaction of the electron, ion and atom in the plasma in the process of the plasma formation. Stark broadening of the Ni atom at the 385.83 nm is measured experimentally, the variation character for Stark broadening with the radial distance is received. Stark broadening and the relative intensity of the spectrum lines increases firstly to its maximum and then decreases along the direction of laser beam when the distance from the target surface increase. The maximum value of Stark broadening and relative intensity of the spectrum lines appear at 1.5 mm from the target surface.

Acknowledgments This work is supported by the National Natural Basic Research Program (973) of China (No. 2012CB214903), civil engineering professional provincial demonstration funding project, Anhui province construction industry science and technology program in 2011(No. 2011YF-04), Association of Chinese coal industry fund project 2011 (No. MTK2011-450).

References

- [1] P. E. Dyer, A. Issa, and P. H. Key, *Appl. Surf. Sci.* 46 (1990) 89.
- [2] J. Hermann, C. Boulmer-Leborgne, and B. Dubreuil, *Appl. Surf. Sci.* 46 (1990) 315.
- [3] X. S. Tang, C. Y. Li, X. H. Gi, *et al.*, *J. At. Mol. Phys.* 21 (2004) 176 (in Chinese).
- [4] S. V. Shabanov and I. B. Gornushkin, *Spectrochim. Acta Part B* 66 (2011) 413.
- [5] Q. M. Xiao, Z. Yao, J. H. Liu, *et al.*, *Thin Solid Films* 519 (2011) 7116.
- [6] J. M. Fan, G. X. Yao, X. Y. Zhang, *et al.*, *Chinese J. Lasers* 37 (2010) 1956.
- [7] Z. W. Wu, B. N. Wan, Q. Zhou, *et al.*, *Plasma. Sci. Technol.* 7 (2005) 2915.
- [8] G. L. Song and Y. Z. Song, *Spectro. Spec. Anal.* 23 (2003) 22.
- [9] R. Fantoni, L. Caneve, F. Colao, *et al.*, *Spectrochim. Acta Part B* 63 (2008) 1097.
- [10] A. M. Alonso, *Spectrochim. Acta Part B* 63 (2008) 598.
- [11] B. Q. Yang, J. Y. Zhang, S. S. Han, *et al.*, *High. Pow. Las. Parti. Bea* 17 (2005) 703.
- [12] A. Elhassan, A. Giakoumaki, D. Anglos, *et al.*, *Spectrochim. Acta Part B* 63 (2008) 504.
- [13] G. C. Wang and Z. J. Zheng, *Chinese J. Lasers* 35 (2008) 524.
- [14] W. Liu, H. L. Xu, G. Méjean, *et al.*, *Spectrochim. Acta Part B* 62 (2007) 76.
- [15] J. Hermann, C. B. Leborgne, B. Dubreuil, *et al.*, *J. Appl. Phys.* 74 (1993) 3071.

- [16] Z. W. Li and J. H. Zhang, *J. At. Mol. Phys.* 28 (2011) 1067 (in Chinese).
- [17] Z. X. Fu, X. Y. Zhang, Q. Li, *et al.*, *J. At. Mol. Phys.* 28 (2011) 1061 (in Chinese).
- [18] F. Zhao, R. H. Li, L. B. Zhou, *et al.*, *J. At. Mol. Phys.* 27 (2010) 107 (in Chinese).
- [19] W. Xiong, Q. Zhang, F. Zhao, *et al.*, *J. At. Mol. Phys.* 27 (2010) 283 (in Chinese).
- [20] Q. L. Ma, V. Motto-Ros, W. Q. Lei, *et al.*, *Spectrochim. Acta Part B* 65 (2010) 896.
- [21] V. Zorba, X. L. Mao, and E. Richard, *Spectrochim. Acta Part B* 66 (2011) 189.
- [22] K. Kodama and K. Wagatsuma, *Spectrochim. Acta Part B* 59 (2004) 429.
- [23] K. Wagatsuma and H. Honda, *Spectrochim. Acta Part B* 60 (2005) 1538.
- [24] J. A. Mckay, R. D. Bleach, D. J. Nagel, *et al.*, *J. Appl. Phys.* 50 (1979) 3231.
- [25] J. T. Knudtson, W. B. Green, and D. G. Sutton. *J. Appl. Phys.* 61 (1987) 4771.
- [26] M. G. Su, G. Y. Cheng, S. D. Zhang, *et al.*, *J. At. Mol. Phys.* 22 (2005) 472 (in Chinese).
- [27] Y. Z. Song, L. Li, and Y. H. Zhang. *J. At. Mol. Phys.* 17 (2000) 221 (in Chinese).